Iranian Journal of Geophysics, Vol 19 No 6, 2026, Page 85 – 104 (Research Article)
DOI: 10.30499/ijg.2025.476758.1629

Spatial reconstruction of geological features distribution based on remote sensing model using convolutional neural network algorithm in Patuha geothermal field, Indonesia

Widya Utama[1*], Ira Mutiara Anjasmara[1], Dhea Pratama Novian Putra[2], Daniel Sahat Rezeki Hutagalung[3], Muhammad Himam Awali[3], Sherly Ardhya Garini[4] and Rista Fitri Indriani[2]

[1] *Associate Professor, Department of Geophysics Engineering, Institut Teknologi Sepuluh Nopember, Surabaya, Indonesia*
[2] *M.Sc., Department of Geomatics Engineering, Institut Teknologi Sepuluh Nopember, Surabaya, Indonesia*
[3] *Bachelor, Department of Geomatics Engineering, Institut Teknologi Sepuluh Nopember, Surabaya, Indonesia*
[4] *Ph.D. Student, Department of Informatics, Institut Teknologi Sepuluh Nopember, Surabaya, Indonesia*

(Received: 04 September 2024, Accepted: 04 January 2025)

Abstract

Recent advancements in remote sensing technology have optimized spatial data by enhancing the resolution of field measurement data. Regional geological maps are still used to validate geoscience models because of their high reliability, which is based on field measurements, but they have relatively low spatial resolution. Combining remote sensing models with machine learning algorithms offers a promising method to reconstruct regional geological maps into high-resolution geological maps, especially in volcanic regions with active geothermal systems such as the Patuha Geothermal Field in Indonesia. Models derived from pre-processed satellite gravity data and normalized satellite images, with standardized pixel raster sizes, form the quantitative basis for reconstructing regional geological map models. The Convolutional Neural Network (CNN) algorithm serves as the computational basis for reconstructing spatial models. The results of spatial reconstruction modeling using remote sensing data provide detailed insights into the distribution of geological features, achieving an accuracy rate of 81.26%. These varying geological feature zones are likely related to the dynamics of active volcanic regions. Since the active volcanic activity, geological fault structures have been formed and could be identified by combination of derivative analysis and remote sensing approach. Second Vertical Derivative (SVD) provides physical characteristics of active fault planes, integrating it with remote sensing analysis to indicate fault planes appeared in the surface. There is a clear correlation between the distribution of reconstructed lithological features and geological fault planes. Areas with a high concentration of fault planes often have a more diverse distribution of geological features, likely due to the influence of active faults, volcanic activity, and material erosion. Adding hyperparameters and geological feature constraints to the machine learning algorithm is a promising option for further research in this area of geological map reconstruction.

Keywords: Geological map, geothermal, machine learning, satellite gravity, satellite imagery

[*]Corresponding author: widya@geofisika.its.ac.id

1 Introduction

Although regional geological maps have high data reliability due to being based on field measurements, they suffer from low spatial resolution (Baker et al., 2013; Fluet-Chouinard et al., 2015; Jaud et al., 2022). This limitation arises from challenges such as varied topography and the vast area of coverage, which often restrict the movement of geologists who are also in limited number (Bishop et al., 2012; Hoggard et al., 2021; Schrott and Sass, 2008). The low resolution of these maps necessitates additional detailed mapping of specific geological features, which is neither effective nor efficient (Sang et al., 2020; Segoni et al., 2020). This challenge poses a fundamental problem for various activities that require geological feature information in their processes.

In the exploration, exploitation, and monitoring processes of geothermal resource, high-resolution detail in geoscience data is crucial, particularly regarding geological features as the basis data (AlGaiar et al., 2024; Buday-Bódi et al., 2022; Hu et al., 2022). High-resolution geological feature information in geothermal fields is closely related to volcanic activities that have complex and dynamic nature as geothermal conceptual models (Oskooi et al., 2014; Letelier et al., 2021; Medici et al., 2023; Utama et al., 2023). To solve these challenges, remote sensing models are applied to enhance the spatial resolution of geological features using machine learning algorithms for quantitative computation in more specific spatial reconstruction processes. Quantitative spatial reconstruction is better approach to simplify the complexity of geological features and remote sensing models in geothermal fields, reducing the bias from multiple interpretations that commonly occur in the qualitative analysis of integrated geoscience data and models (Wagner and Uhlemann, 2021; Medici et al., 2023; Thiele et al., 2024; Utama et al., 2024; Cao et al., 2024).

Quantitative approach to spatial reconstruction of geological features involves statistical and correlation analysis between recent geological features (e.g., features derived from regional geological maps) and remote sensing data that represent actual surface conditions (Cao et al., 2024; Harishidayat et al., 2022). Machine learning algorithm, specifically Convolutional Neural Network (CNN), becomes architectural computation basis to integrate data and models in this research. CNN algorithm is inspired by biological neural networks, processing multiple input data points to produce a single final decision as output (Qian et al., 2021; Saadi et al., 2022; Shah et al., 2023). It utilizes a convolutional approach, which mathematically matches data correlations to generate final prediction values for each pixel in the model (Su et al., 2021; Vu and Jardani, 2021; Saadi et al., 2022). Therefore, recent geological features and remote sensing data integration can be optimized more effectively using the CNN algorithm.

The CNN algorithm for spatial reconstruction in geological features with remote sensing data as a resolution-enhancing factor has already been applied in several research. Most of the research about geological reconstruction from remote sensing data and machine learning algorithm has been conducted in arid regions (e.g., desert, tundra, savannah) to avoid vegetation coverage issues that complicate surface lithology identification (Cracknell and Reading, 2014; El Fels and El Ghorfi, 2022; Shirmard et al., 2022; Han et al., 2022, 2023; Chi et al., 2023; EL-Omairi and El Garouani, 2023;

Eskandari et al., 2023; Mahboob et al., 2024; Wang et al., 2024). Furthermore, to classify the surface geological features, each research utilized different satellite imagery band combinations, based on their specific material contents interpretation (e.g., iron, sulfur, silica) (Harvey and Fotopoulos, 2016; Shirmard et al., 2022; Chi et al., 2023; Eskandari et al., 2023; Mahboob et al., 2024; Wang et al., 2024).

These challenges become more complex when geological feature reconstruction is applied to Indonesia's geothermal areas, which are predominantly covered by dense vegetation. Dynamic surface material exposure, caused by volcanic activity and disaster-prone conditions (e.g., landslides, earthquakes, forest fires), further contributes to rapid changes in surface material visibility (Utama et al., 2023; Prasetya, 2024; Putra et al., 2024). A novel approach combining low-frequency with high wavelength satellite imagery bands, which are believed could penetrate vegetation coverage deeper, simultaneously with related physical properties models from satellite gravity data could address these challenges and improve geological feature reconstruction in Indonesia's geothermal fields.

Patuha Geothermal Field is an active geothermal system located in the western part of Java Island, Indonesia. Recent geoscience research in the Patuha Geothermal Field has primarily focused on the geothermal reservoir and surface manifestations (Rahayudin et al., 2020; Ramadhan et al., 2022; Sondakh, 2022; Kusumasari et al., 2024;). Additionally, studies have been conducted on field geological mapping, groundwater recharge area, hydrothermal dynamics, and fault interpretation (Rahayudin et al., 2020; Sondakh, 2022; Putra, 2024; Reski et al., 2024). However, no research has attempted to reveal unidentified features in a high-resolution spatial reconstructed surface geological model.

This research aims to enhance the spatial resolution of geological feature distribution by integrating remote sensing models with the physical properties of each geological feature at the Patuha Geothermal Field. Fig. 1 depicts the research area that covered the Patuha Geothermal Field and its surrounding area. Recent geological features, as represented by a regional geological map, will be integrated with remote sensing data for spatial reconstruction using a CNN algorithm, resulting in a high-resolution predicted map of geological feature distribution. Related geological structure in the form of geological fault, also be interpreted using satellite gravity models to refine the analysis. The focus on Indonesia's geothermal field represents a novelty to address challenges such as dense vegetation coverage and the rapid changes in exposed surface materials.

2 Geological review

The Patuha Geothermal Field is located in geological weak area of Quaternary volcanic zones, which may indicate potential surface geological structure dynamics that affect the spatial detailing of geological features (Intani et al., 2020; Gutiérrez-negrín, 2024; Putra, 2024). Based on regional geological genesis, this area is composed by volcanic product activity from Quaternary volcanoes surrounding its area (Ratman and Gafoer, 1998; Kusdji et al., 2013). There are Holocene Rock Formation covering older rock formation from Pleistocene epoch (Ratman and Gafoer, 1998; Kusdji et al., 2013). It means if this area is covered by relatively young material from volcanic activity in Quaternary period.

Several igneous rocks (e.g., andesite,

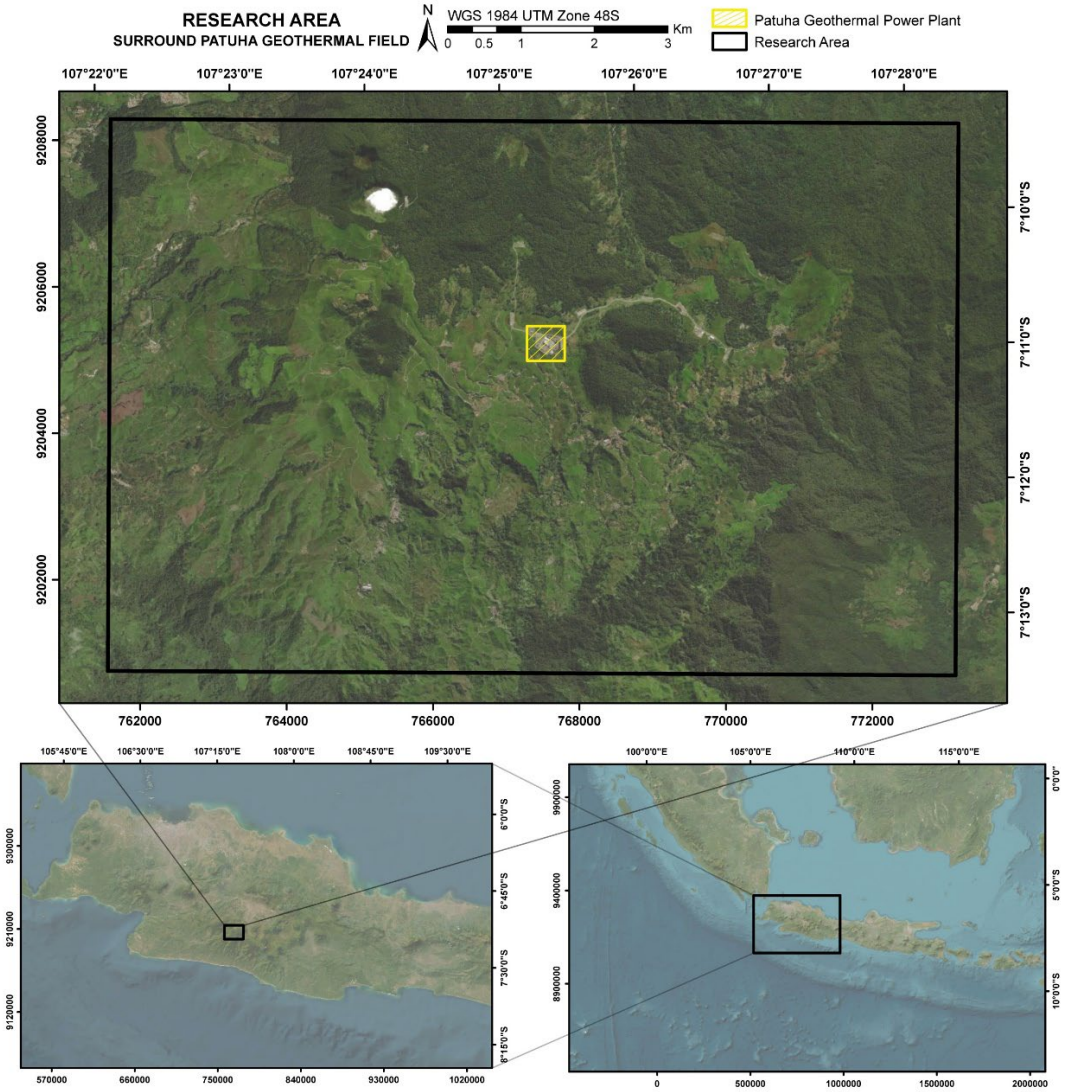

Figure 1. Research area. Patuha Geothermal Field is located in the western part of Java Island, Indonesia, which is part of the Quaternary volcanic mountain belt that extends from west to east across the island identified in the Patuha Geothermal Field area.

basalt) and pyroclastic material (e.g., volcanic breccia, tuff, lahar) covered the surface of Patuha Geothermal Field (Ratman and Gafoer, 1998; Kusdji et al., 2013). Lahar and Lava Formation from Mount Kendeng in the eastern part of research area is known as the oldest, while Lava Formation from Mount Patuha has identified as the youngest from its source in the north (Kusdji et al., 2013). Lava material would formed igneous rock, while pyroclastic deposits had lithification process into pyroclastic rock (Kusdji et al., 2013). Fig. 2 displays the regional geological features of the Patuha Geothermal Field.

As active Quaternary volcanic area, this area had various geological structures, such as joint, fracture, fault, and folds that indicated as geological weak zone (Putra, 2024). Volcanic products distributed across the Patuha Geothermal Field indicate as active volcanic zone. They are relatively new formed, so the geothermal heat source is

potentially still having sufficiently high temperatures for the geothermal energy extraction process (Wang and Pang, 2023). This geothermal energy is actively exploited for geothermal power plant in Patuha Geothermal Field until now.

3 Methodology

Methodology of this research consists of four main stages: pre-processing; computational model reconstruction; accuracy assessment; interpretation and analysis. Preprocessing stage is specifically divided into two main steps: remote sensing models normalization and spatial raster pixels definition. Each remote sensing model, as outlined in Table 1, corresponds to the physical properties of geological features. Regional geological features derived from the geological map are as foundation of the spatial reconstruction process. Complete Bouguer Anomaly (CBA) values and rock density distributions are directly associated with gravity characteristics and specific density of each geological feature (Guglielmetti and Moscariello, 2021; Putra, 2021; Mulugeta et al., 2021; Nigussie et al., 2023).

Models derived from Landsat-8 satellite imagery represent surface lithology distribution and land cover influence on geological features within the Patuha Geothermal Field. Low-frequency bands with high wavelength, such as Near Infrared (NIR) and Shortwave Infrared (SWIR) are predominantly used in band ratio analysis because of their ability to penetrate vegetation canopies and reveal surface lithology (Yusroni et al., 2021; Riefolo et al., 2022; Utama et al., 2023; Putra et al., 2024). Low-frequency with high wavelength satellite imagery bands are crucial in revealing surface lithology conditions while identifying the land cover characteristics. Surface lithology properties derived from band ratio analysis are classified into three categories based on their weighting (Putra, 2024). Low-weighted lithology is associated with short vegetation distribution and identified using the NIR and Visual Red band ratio (Aliyan et al., 2022; Putra et al., 2024; Utama et al., 2024). Medium weighted lithology corresponds to tall vegetation distribution and is interpreted through the SWIR and NIR band ratio (Aliyan et al., 2022; Putra et al., 2024; Utama et al., 2024). High-weighted lithology is linked to built-up land areas, identified using the SWIR and Visual Blue band ratio (Aliyan et al., 2022; Putra et al., 2024; Utama et al., 2024). Furthermore, Land Surface Temperature (LST) is calculated from the Thermal Infrared Sensor (TIRS) band, integrating satellite brightness and vegetation emissivity measurements to provide temperature distribution of surface lithology conditions (Muzaky and Jaelani, 2019).

Table 1. Remote sensing models related to the specific physical properties of geological features.

Dataset	Data	Source
Geological Map	Geological Feature	Geological Agency of Republic of Indonesia with modification (Kusdji et al., 2013)
Satellite Gravity Model	Complete Bouguer Anomaly	Global Gravity Model Plus (GGMPLus) (Hirt et al., 2013) with several data processes
	Rock Density	
Satellite Imagery	Red 5/4	Landsat 8 OLI (United States Geological Survey, 2013) with several data processes
	Green 6/5	
	Blue 7/2	
	Land Surface Temperature	

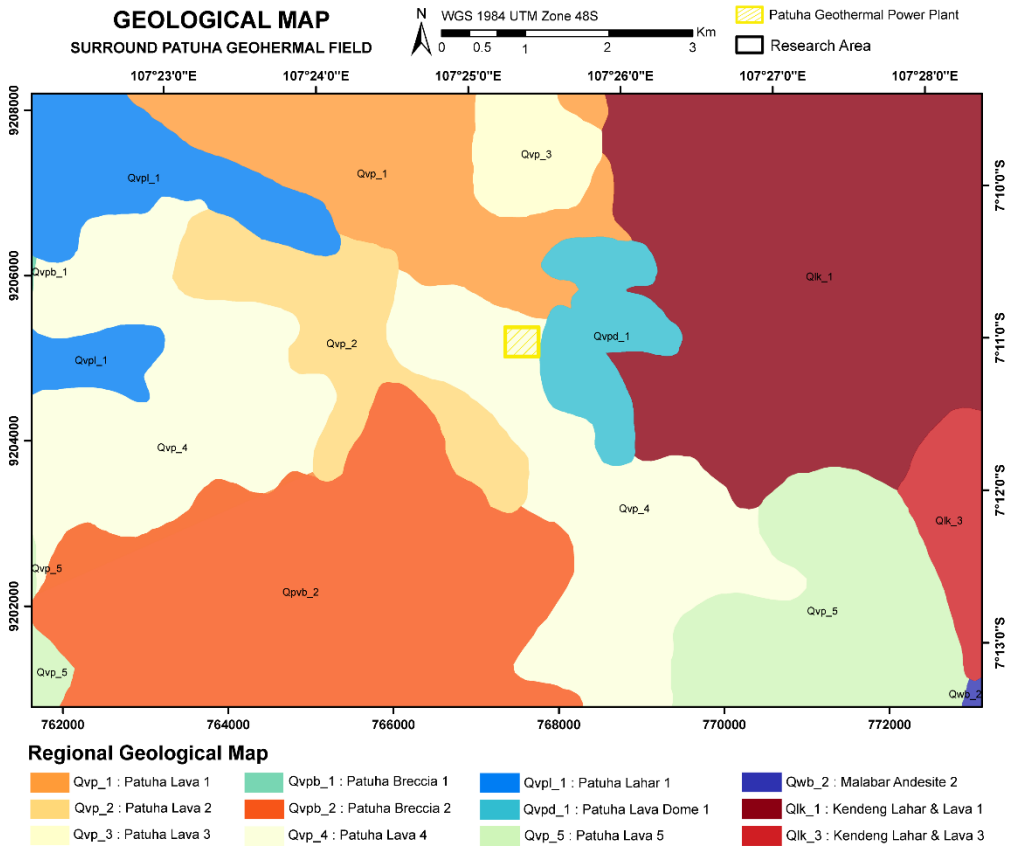

Figure 2. Geological features distribution in Patuha Geothermal Field. Lava and pyroclastic products from Mount Patuha are dominated by the younger geological age rather than products from Mount Malabar and Mount Kendeng in the east (Kusdji et al., 2013).

Due to the diverse values range exhibited by physical properties, normalization is crucial to ensure that each model has a balanced influence on the reconstruction process. Normalization is performed by scaling all physical property models obtained from remote sensing data to a range of 0–1, as written in Eq. (1), where x' is normalized value, x is actual value, $\min(x)$ is minimum value of the range, and $\max(x)$ is maximum value of the range (Aksu et al., 2019; Singh and Singh, 2020).

$$x' = \frac{x - \min(x)}{\max(x) - \min(x)} \quad (1)$$

Defining spatial raster pixels for each physical property model is essential to streamline computational processes. The variation in raster pixel resolution among different remote sensing datasets affects the resolution of their corresponding physical property models (e.g., a 200-meter resolution for satellite gravity data results in a 200-meter resolution for CBA and rock density models, while a 30-meter resolution for satellite imagery data produces a 30-meter resolution for band ratio models). To address these resolution differences, raster pixel definition has been standardized to ensure uniform resolution across all physical property models and geological features model. In this research, a 15-meter raster pixel resolution was adopted, as it is half of the best resolution among the input data (30 meters from satellite imagery data), where this approach allows the predicted reconstruction model to achieve higher spatial resolution.

Normalized and raster pixel defined physical properties model simultaneously

with classified geological features would be inputted into computational model reconstruction process. Computation and visualization of model reconstruction are based on the Convolutional Neural Network (CNN) machine learning algorithm. CNN algorithm operates on principles similar to the neural networks of living organisms as combining and processing information from several simple input models to create a more complex output model (Kattenborn et al., 2021; Miao et al., 2021; Mishra et al., 2021).

Using Python programming language, the CNN architecture leverages the TensorFlow library for its robust features and deep learning flexibility. Effectiveness in image transformation and pattern recognition to produce advanced model prediction from convolutional equation concept is the main advantage of CNN algorithm for model reconstruction (Abiodun et al., 2019; Puzyrev, 2019). However, due to the large number of intercorrelated features involved in convolutional calculations, the CNN algorithm typically requires more computational time compared to other commonly used machine learning algorithms for spatial reconstruction, such as Random Forest and K-Nearest Neighbor (Zhang et al., 2019; Alzubaidi et al., 2021).

Accuracy assessment serves as the evaluation of the predicted model's representation of actual field conditions (Cracknell and Reading, 2014). It is crucial to base accuracy values on their alignment with field data representation (Bishop et al., 2012; Cracknell and Reading, 2014; Harvey and Fotopoulos, 2016; Han et al., 2022; Putra et al., 2024). Regional geological map of Patuha Geothermal Field is considered as representative of field data derived from geological field surveys.

Interpretation and analysis of the spatial reconstruction model include additional information to enhance understanding and support the geological feature reconstruction result. Interpreted fault structure data is crucial for analyzing potential distributions and gaining insights into the reconstructed spatial model developed. Geological fault structures were derived from satellite gravity data processing, specifically using the Second Vertical Derivative (SVD) of the CBA values (Putra, 2021). Additionally, the location of research area within tropical region is characterized by active volcanic processes providing further context and depth to the interpretation and analysis of the reconstruction model. The overall workflow of this research is illustrated in Fig. 3.

4 Results and discussion

Pre-processing results revealed significant differences in the ranges of data values, which varied substantially between original range value and required uniformity. As shown in Table 2, the Complete Bouguer Anomaly (CBA) values range from -252.5078 to 24.1387 mGal, whereas rock density values span only from 2.4936 to 3.0182 g/cm³. Furthermore, differences in decimal precision posed challenges during the pre-processing stage; for instance, the satellite gravity model product had a precision of four decimal places, while the satellite imagery model product was limited to two decimal places.

To address these imbalances, normalizing the data to a consistent range was implemented as an effective strategy to equalize the influence of each model parameter (Zhao et al., 2020; Ahmadzadeh et al., 2021). Following Eq. (1), the normalization process adjusts each parameter, i.e., the lowest actual value is set to zero and the highest value to one, while preserving the original distribution. This ensures that intermediate parameter values are proportionally scaled within the normalized range. The value ranges before and after normalization are summarized in Table 2.

Table 2. The range of data values before and after normalization.

Data	Unit	Before Normalization	After Normalization
Geological Feature	-	no value	0 - 1
Complete Bouguer Anomaly	mGal	-252.5078 to 24.1387	0 - 1
Rock Density	gr/cm^3	2.4936 – 3.0182	0 - 1
Band Ratio Red 5/4	-	0.57 – 3.22	0 - 1
Band Ratio Green 6/5	-	0.47 – 1.61	0 - 1
Band Ratio Blue 7/2	-	0.34 – 2.21	0 - 1
Land Surface Temperature	ºC	28.37 – 53.64	0 - 1

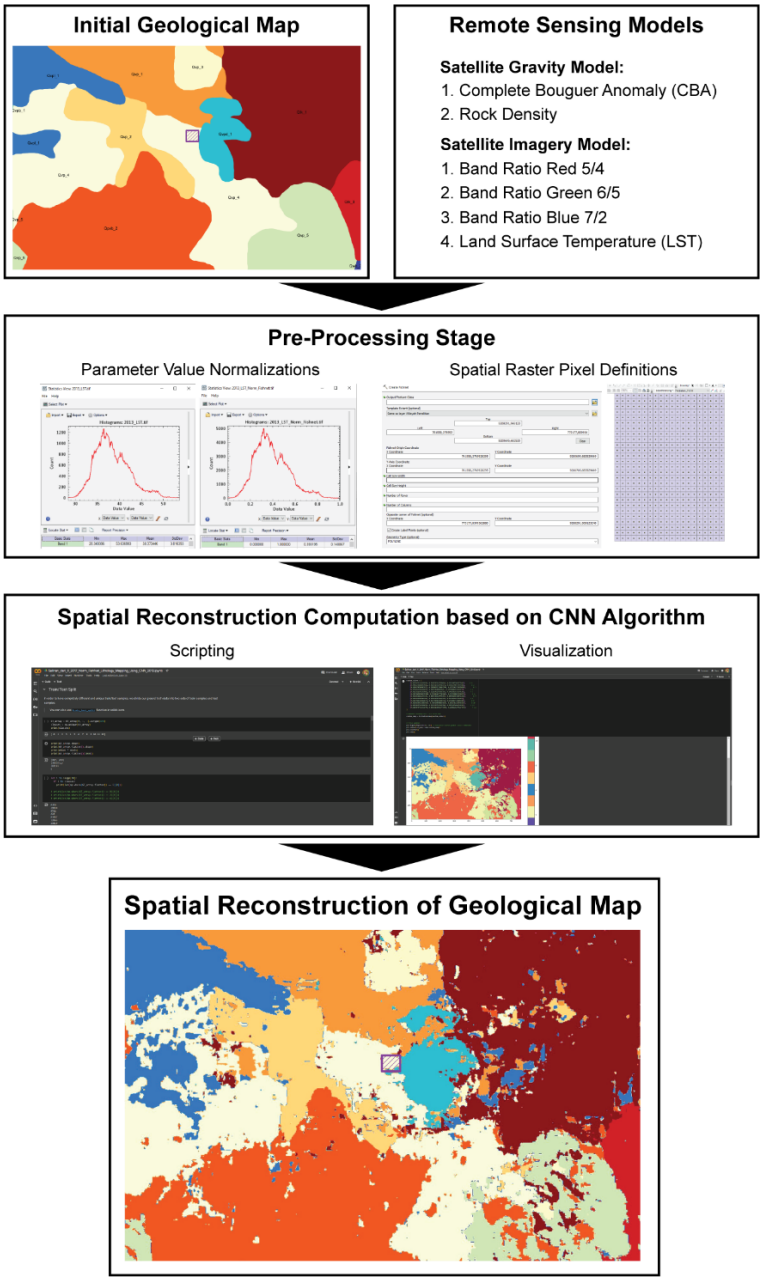

Figure 3. Research flowchart. Regional geological features map and physical properties model are utilized in the pre-processing stage for data normalization and raster pixel definition, integrated into scripting and visualization for model reconstruction with accuracy calculations, and concluded with interpretation and analysis.

Observation of the value ranges for geological feature model parameters in Table 2 reveals that no single value range precisely represents the distribution of geological features. However, deep learning algorithms like CNN require well-defined and consistent values for each model parameter to perform spatial reconstruction calculations effectively (Novaes et al., 2021). To address this issue, the geological features characteristics were used as reference points to determine exact values for spatial reconstruction computations.
The relative age sequence of lithological units was used as a key feature, where the oldest lithology was assigned the lowest value, and progressively younger rocks were assigned higher values, with the youngest lithology receiving the highest value. This approach is based on the principles of lithological superposition and inclusion in stratigraphy, which state that the oldest lithology typically forms the lowest layer and is less prominent on the Earth's surface. Otherwise, younger lithologies, which overlie older formations, are more visible on the surface and thus assigned higher priority. This stratigraphic framework ensures a logical and systematic determination of exact values for geological features in the spatial reconstruction process.

Spatial raster data was used to simplify the calculation of model reconstruction values because each pixel represents specific values for each input model parameter. This necessitates the conversion of model parameters that are still in vector data format into raster format, as in the case of the geological feature parameter. This conversion is essential to spatially define geological features in raster data format, similar to how other model parameters have already been represented.

The variation in pixel sizes of spatial raster data presents a problem as urgent as the variation in the ranges of model parameters. Standardizing pixel sizes is crucial to potential computational issue in predicting model (Burgueño et al., 2023; Xu et al., 2023). This standardization is achieved using fishnet analysis combined with multi-value extraction techniques, which create a consistent spatial pixel size without reducing the variation of the previously normalized model parameter values. Table 3 shows the variation in raster sizes before and after the pixel size standardization process.

The scripting stage involves writing the computational script for CNN architecture, consisting of a set of commands and programming library that are integrated each other. This script acts as a bridge between the handling of input data and the reconstruction modules. The scripting process for spatial reconstruction includes several key steps: data and libraries input, train/test splitting, data standardization, feature classification, and accuracy assessment. These steps are interconnected, requiring the script to meet the requirements of each stage to ensure smooth operation.

The inputting of data and libraries involves two main components that initiate the spatial reconstruction computation process: the initial data input and the input of CNN algorithm modules for spatial reconstruction. The initial data consists of models that have already been through the pre-processing stage. After all the data inputs are incorporated into the computational process, the relevant library based on the CNN algorithm needs to be inputted for spatial reconstruction.

The train/test splitting stage involves dividing sample points from the input data raster pixels to classify them as either training data or testing data. In this research, 70% of the total samples are used as training data to serve as a reference for the machine learning algorithm in identifying patterns and predicting the model. The remaining 30% of the samples are used as testing data to validate predictions and to assess the model's reconstruction accuracy. Training data typically includes

more samples than testing data because the complexity of each model parameter requires a larger training set to achieve a representative model prediction that aligns with the distribution patterns of each parameter's values (Tut Haklidir and Haklidir, 2020; Mordensky et al., 2022).

Table 3. Variation in pixel size of spatial raster data before and after standardizing the raster size.

Data	Unit	Before Standardization	After Standardization
Geological Feature	m	vector format	15 x 15
Complete Bouguer Anomaly	m	200 x 200	15 x 15
Rock Density	m	200 x 200	15 x 15
Band Ratio Red 5/4	m	30 x 30	15 x 15
Band Ratio Green 6/5	m	30 x 30	15 x 15
Band Ratio Blue 7/2	m	30 x 30	15 x 15
Land Surface Temperature	m	100 x 100	15 x 15

Each geological feature is included in both the training and testing datasets to ensure that their physical characteristics are accurately represented in the spatial reconstruction model predictions. The correlation between geological features and their physical properties is the pattern recognized by the CNN architecture to generate a new predicted model using a statistical approach. This statistical approach is achieved through the standardization applied in the CNN algorithm.

Data standardization involves statistical methods to adjust the data distribution pattern, ensuring the data follows a normal distribution. Normal distribution is crucial in statistical modeling because it helps represent the model accurately with minimal outliers, thereby reducing noise in the model (Jiao et al., 2023; Grubov et al., 2024). Spatial reconstruction process in this research includes data standardization that consists of two main steps: transforming the data to align the meaning with a normal distribution and applying a specific scale division to minimize the effect of outliers. Together, these steps ensure that the model parameters exhibit a normal distribution pattern with minimal impact from outliers.

Feature classification in the spatial reconstruction using the CNN algorithm involves categorizing the spatial features to be reconstructed and calculating the model predictions (Kattenborn et al., 2021). In this research, the spatial feature classes are geological features that serve as fundamental model parameters, reconstructed based on the influence of other model distributions. There are 12 geological features representing the lithological conditions of the study area's rock formations, which are the spatial features examined in this study. After classification, these geological features proceed to the model prediction stage, where the reconstruction model is calculated to represent a combination of all models.

To evaluate the accuracy of the spatial reconstruction model predictions, an accuracy assessment is conducted to determine the accuracy level of the model. Predicted model accuracy is assessed by comparing the model's predictions on testing data points with an evaluation model, which is assumed to represent the actual data (Duplyakin et al., 2022; Putra et al., 2023; Utama et al., 2023). The evaluation model is derived from the sample points of the testing data on the distribution parameters of geological features obtained during the training/testing phase (Cracknell and Reading, 2014). A match between the model predictions and the evaluation model indicates that the predictions are ac-

curate. The accuracy assessment in this research showed that the spatial reconstruction model for geological features achieved an accuracy of 81.26%, suggesting that the model predictions effectively represent the distribution of geological features in the Patuha Geothermal Field with a higher spatial resolution of 15-meters.

The visualization stage presents models of lithological features and other physical property parameters, allowing for a clear comparison of spatial data distribution and resolution before and after the reconstruction process. During this stage, in-depth analysis is conducted to compare the models, highlighting the differences before and after reconstruction. Fig. 4 illustrates this comparison of the predicted models for the spatial reconstruction of geological features in the study area. An increase in spatial resolution is evident, marked by the appearance of relatively narrow features that fill the gaps between more widely distributed geological features. This indicates that the spatial reconstruction process for geological features in the Patuha Geothermal Field has been successful, producing more detailed results.

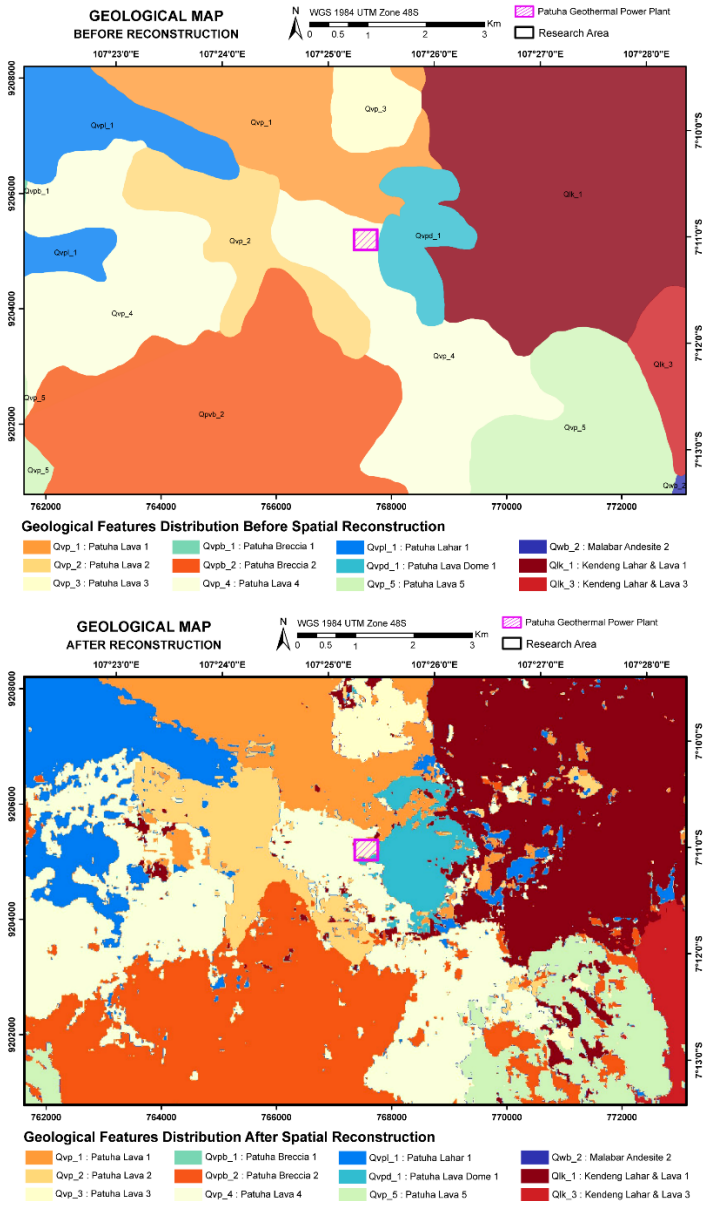

Figure 4. Distribution of geological features before (above) and after (below) spatial reconstruction using the CNN algorithm.

The increased spatial resolution of the geological map facilitates a deeper analysis of the causes behind the relatively more "scattered" distribution of geological features compared to the distribution before reconstruction. This "scattered" pattern observed in the spatially reconstructed geological features is related to the dynamics within the geothermal field, an active volcanic area with a steep slope gradient. The volcanic activity in the Patuha Geothermal Field is primarily driven by Mount Patuha, which remains a part of the Quaternary-aged Mountain Belt. Being within an active volcanic zone, interpreted geological faults are scattered throughout the research area, which is illustrated in Fig. 5.

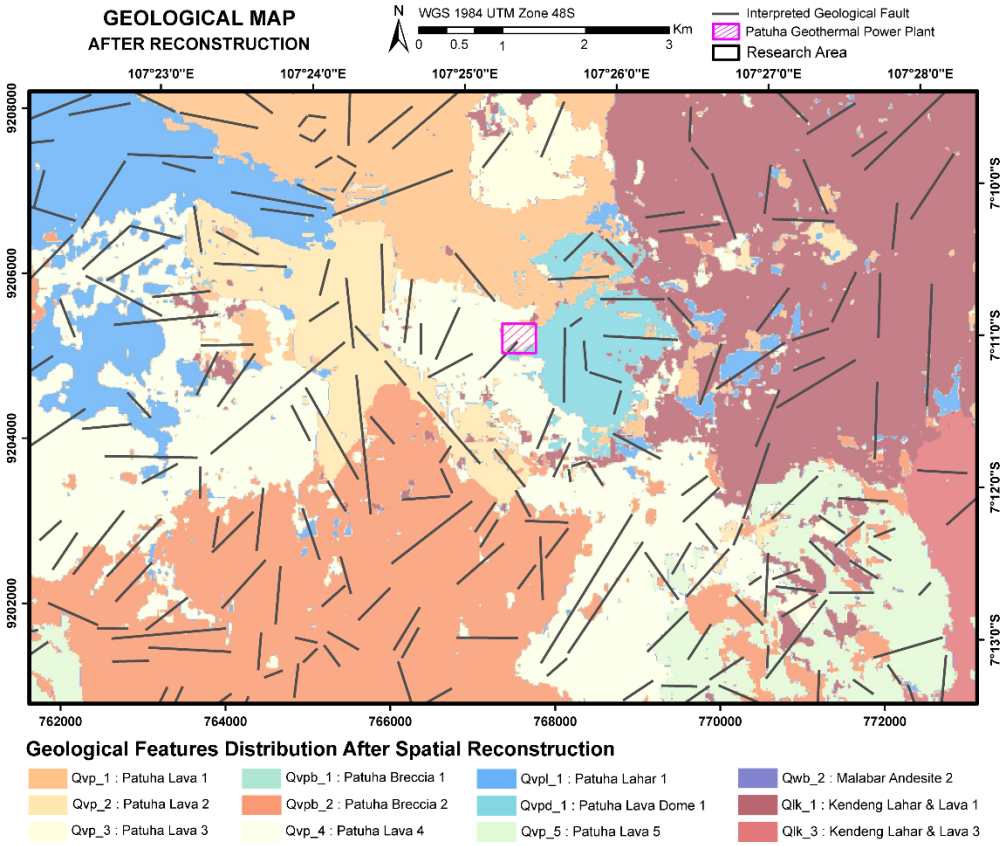

Figure 5. The scattered pattern in the distribution of geological features from the spatial reconstruction results, showing an interconnected distribution with interpreted geological faults.

Geological fault interpretation to analyze "scattered" feature patterns was derived from the satellite gravity data analysis. CBA values from satellite gravity data need to be derived twice to obtain the second derivative of their extreme values (Putra, 2021; Hofi et al., 2024). This second derivative shows contrasts between high and low anomalies, which indicate the presence of geological fault planes (Putra, 2021; Hofi et al., 2024). The interpreted geological faults, further identified through lineament analysis from Digital Elevation Model (DEM), are considered active faults, based on the ability of the faults to deform Quaternary material, including both lava flows and pyroclastic deposits (Putra, 2024; Silva-Fragoso et al., 2024).

In the geothermal fields context, geological faults distribution tends to relatively random pattern, unlike the more structured faults formed by tectonic activity (e.g., Baribis-Kendeng Fault across Java Island and Semangko Fault across Sumatra Island), which consist of multiple

fault segments combining to form larger fault systems. This randomness in fault patterns, particularly in the Patuha Geothermal Field, significantly influences surface lithology dynamics. Additionally, the dominant volcanic and structurally mountainous morphology of the region increases its susceptibility to erosion and landslides. These geological phenomena affect inclusion stratigraphy, which is reflected in the predicted reconstruction model visualization.

5 Conclusion

Spatial resolution enhancement of geological feature distributions in the Patuha Geothermal Field is derived through the spatial reconstruction of regional geological features using Convolutional Neural Network (CNN) algorithm. The method integrates geological feature distributions with physical property models to generate more detailed and accurate geological feature distributions. This research introduces a novel approach to address challenges such as dense vegetation coverage and the rapid changes in exposed surface materials. By combining low-frequency with high wavelength satellite imagery bands, which can penetrate vegetation more effectively, combined with physical property models derived from satellite gravity data, this method significantly improves the accuracy of geological feature reconstruction in the Patuha Geothermal Field.

The reconstruction process begins with pre-processing steps, such as normalizing the model value ranges and defining the raster pixel size, which are fundamental for preparing the input data for the CNN algorithm. In addition, scripting and visualization are critical components that facilitate the integration of all physical property model parameters within the CNN algorithm. This comprehensive approach results in a geological feature distribution model with a higher spatial resolution, achieving an accuracy of 81.26% in the reconstructed model.

There is a notable correlation between the distribution of reconstructed lithological features and the distribution of geological fault planes. Zones with a high concentration of geological fault planes often show a more varied distribution of geological features. This variation is related to the active geological faults, which significantly influences the dynamics of geological features in the study area, alongside the effects of volcanic activity and material erosion. Overall results of this research illustrate potential inclusion stratigraphy in the Patuha Geothermal Field can be effectively identified through the spatial reconstruction of geological features.

Acknowledgements

The author expresses sincere gratitude for the cooperation of all parties that enabled the completion of this scientific article. This research was funded by the ITS Scientific Research Program at Institut Teknologi Sepuluh Nopember (ITS), under researcher contract number 1135/PKS/ITS/2024, dated 29 February 2024.

References

Abiodun, O. I., Jantan, A., Omolara, A. E., et al., 2019, Comprehensive review of artificial neural network applications to pattern recognition: IEEE Access, **7**, 158820–158846, https://doi.org/10.1109/ACCESS.2019.2945545.

Ahmadzadeh, A., Aydin, B., Georgoulis, M. K., Kempton, D. J., Mahajan, S. S., and Angryk, R. A., 2021, How to train your flare prediction model: revisiting robust sampling of rare events: The Astrophysical Journal Supplement Series, **254**(2), 23, https://doi.org/10.3847/1538-4365/abec88.

Aksu, G., Guzeller, C. O., and Eser, M. T., 2019, The effect of the normalization

method used in different sample sizes on the success of artificial neural network model: International Journal of Assessment Tools in Education, **6**(2), 170–192, https://doi.org/10.21449/ijate.479404.

AlGaiar, M., Hossain, M., Petrovski, A., Lashin, A., and Faisal, N., 2024, Applications of artificial intelligence in geothermal resource exploration: A review: Deep Underground Science and Engineering, **3**(3), 269–285, https://doi.org/10.1002/dug2.12122.

Aliyan, S. A., Bratanegara, A. S., Ihsan, H. M., Astari, A. J., and Somantri, L., 2022, Identification of lithological characteristics using multispectral Landsat 8 Oli Imagery in the Cipatujah Area, West Java, Indonesia: IOP Conference Series: Earth and Environmental Science, **1089**(1), https://doi.org/10.1088/1755-1315/1089/1/012021.

Alzubaidi, L., Zhang, J., Humaidi, A. J., et al., 2021, Review of deep learning: concepts, CNN architectures, challenges, applications, future directions: Journal of Big Data, **8**(1), Springer International Publishing, https://doi.org/10.1186/s40537-021-00444-8.

Baker, B. A., Warner, T. A., Conley, J. F., and McNeil, B. E., 2013, Does spatial resolution matter? A multi-scale comparison of object-based and pixel-based methods for detecting change associated with gas well drilling operations: International Journal of Remote Sensing, **34**(5), 1633–1651, https://doi.org/10.1080/01431161.2012.724540.

Bishop, M. P., James, L. A., Shroder, J. F., and Walsh, S. J., 2012, Geospatial technologies and digital geomorphological mapping: Concepts, issues and research: Geomorphology, **137**(1), 5–26, https://doi.org/10.1016/j.geomorph.2011.06.027.

Buday-Bódi, E., Irfan, A., McIntosh, R. W., et al., 2022, Subregion-scale geothermal delineation based on image analysis using reflection seismology and well data with an outlook for land use: Sustainability (Switzerland), **14**(6), https://doi.org/10.3390/su14063529.

Burgueño, A. M., Aldana-Martín, J. F., Vázquez-Pendón, M., et al., 2023, Scalable approach for high-resolution land cover: a case study in the Mediterranean Basin: Journal of Big Data, **10**(1), https://doi.org/10.1186/s40537-023-00770-z.

Cao, X., Liu, Z., Hu, C., Song, X., Quaye, J. A., and Lu, N., 2024, Three-dimensional geological modelling in Earth science research : An in-depth review and perspective analysis: Minerals, **14**(7), 686, https://doi.org/10.3390/min14070686.

Chi, H., Sun, J., Zhang, C., and Miao, C., 2023, Remote sensing data processing and analysis for the identification of geological entities: Acta Geophysica, **71**(3), 1565–1577, https://doi.org/10.1007/s11600-022-00871-y.

Cracknell, M. J., and Reading, A. M., 2014, Geological mapping using remote sensing data: A comparison of five machine learning algorithms, their response to variations in the spatial distribution of training data and the use of explicit spatial information: Computers and Geosciences, **63**, 22–33, https://doi.org/10.1016/j.cageo.2013.10.008.

Duplyakin, D., Beckers, K. F., Siler, D. L., Martin, M. J., and Johnston, H. E., 2022, Modeling subsurface performance of a geothermal reservoir using machine learning: Energies, **15**(3), https://doi.org/10.3390/en15030967.

El Fels, A. E. A., and El Ghorfi, M., 2022,

Using remote sensing data for geological mapping in semi-arid environment: a machine learning approach: Earth Science Informatics, **15**(1), 485–496, https://doi.org/10.1007/s12145-021-00744-w.

EL-Omairi, M. A., and El Garouani, A., 2023, A review on advancements in lithological mapping utilizing machine learning algorithms and remote sensing data: Heliyon, **9**(9), e20168, https://doi.org/10.1016/j.heliyon.2023.e20168.

Eskandari, A., Hosseini, M., and Nicotra, E., 2023, Application of satellite remote sensing, UAV-geological mapping, and machine learning methods in the exploration of podiform chromite deposits: Minerals, **13**(2), https://doi.org/10.3390/min13020251.

Fluet-Chouinard, E., Lehner, B., Rebelo, L. M., Papa, F., and Hamilton, S. K., 2015, Development of a global inundation map at high spatial resolution from topographic downscaling of coarse-scale remote sensing data: Remote Sensing of Environment, **158**, 348–361, https://doi.org/10.1016/j.rse.2014.10.015.

Grubov, V. V., Nazarikov, S. I., Kurkin, S. A., Utyashev, N. P., Andrikov, D. A., Karpov, O. E., and Hramov, A. E., 2024, Two-stage approach with combination of outlier detection method and deep learning enhances automatic epileptic seizure detection: IEEE Access, **12**(September), 122168–122182, https://doi.org/10.1109/ACCESS.2024.3453039.

Guglielmetti, L., and Moscariello, A., 2021, On the use of gravity data in delineating geologic features of interest for geothermal exploration in the Geneva Basin (Switzerland): prospects and limitations: Swiss Journal of Geosciences, **114**(1), https://doi.org/10.1186/s00015-021-00392-8.

Gutiérrez-negrín, L. C. A., 2024, Evolution of worldwide geothermal power 2020–2023: Geothermal Energy, **12**(14), https://doi.org/10.1186/s40517-024-00290-w.

Han, W., Li, J., Wang, S., Zhang, X., Dong, Y., Fan, R., Zhang, X., and Wang, L., 2022, Geological remote sensing interpretation using deep learning feature and an adaptive multisource data fusion network: IEEE Transactions on Geoscience and Remote Sensing, **60**, 1–14, https://doi.org/10.1109/TGRS.2022.3183080.

Han, W., Zhang, X., Wang, Y., et al., 2023, A survey of machine learning and deep learning in remote sensing of geological environment: Challenges, advances, and opportunities: ISPRS Journal of Photogrammetry and Remote Sensing, **202**(December 2022), 87–113, https://doi.org/10.1016/j.isprsjprs.2023.05.032.

Harishidayat, D., Al-Shuhail, A., Randazzo, G., Lanza, S., and Muzirafuti, A., 2022, Reconstruction of land and marine features by seismic and surface geomorphology techniques: Applied Sciences (Switzerland), **12**(19), https://doi.org/10.3390/app12199611.

Harvey, A. S., and Fotopoulos, G., 2016, Geological mapping using machine learning algorithms: International Archives of the Photogrammetry, Remote Sensing and Spatial Information Sciences - ISPRS Archives, **41**(July), 423–430, https://doi.org/10.5194/isprsarchives-XLI-B8-423-2016.

Hirt, C., Claessens, S., Fecher, T., Kuhn, M., Pail, R., and Rexer, M., 2013, New ultrahigh-resolution picture of Earth's gravity field: Geophysical Research

Letters, **40**(16), 4279–4283, https://doi.org/10.1002/grl.50838.

Hofi, L. N., Maryanto, S., Susilo, A., and Wuryani, S. D., 2024, Derivative analysis of gravity data in revealing the subsurface fault structure nodel in Semeru Volcano, East Java and its surrounding: Trends in Sciences, **21**(9), Manuscript, https://doi.org/10.48048/tis.2024.8050.

Hoggard, M., Austermann, J., Randel, C., and Stephenson, S., 2021, Observational estimates of dynamic topography through space and time: Mantle Convection and Surface Expressions, May 2020, 373–411, https://doi.org/10.1002/9781119528609.ch15.

Hu, Y., Cheng, H., and Tao, S., 2022, Opportunity and challenges in large-scale geothermal energy exploitation in China: Critical Reviews in Environmental Science and Technology, **52**(21), 3813–3834, https://doi.org/10.1080/10643389.2021.1971004.

Intani, R. G., Golla, G. U., Syaffitri, Y., et al., 2020, Improving the conceptual understanding of the Darajat Geothermal Field: Geothermics, **83**(August 2019), 101716, https://doi.org/10.1016/j.geothermics.2019.101716.

Jaud, M., Geoffroy, L., Chauvet, F., Durand, E., and Civet, F., 2022, Potential of a virtual reality environment based on very-high-resolution satellite imagery for structural geology measurements of lava flows: Journal of Structural Geology, **158**(March), 104569, https://doi.org/10.1016/j.jsg.2022.104569.

Jiao, Y., Tan, Z., Zhang, D., and Zheng, Q. P., 2023, Short-term building energy consumption prediction strategy based on modal decomposition and reconstruction algorithm: Energy and Buildings, **290**(January), 113074, https://doi.org/10.1016/j.enbuild.2023.113074.

Kattenborn, T., Leitloff, J., Schiefer, F., and Hinz, S., 2021, Review on convolutional neural networks (CNN) in vegetation remote sensing: ISPRS Journal of Photogrammetry and Remote Sensing, **173**(December 2020), 24–49, https://doi.org/10.1016/j.isprsjprs.2020.12.010.

Kusdji, Mawardi, S., Miharnanto, Daryantoni, D., H., L., S., Y., Ipranto, and Sidarto., 2013, Peta Geologi Hasil Interpretasi Citra Inderaan Jauh Ciwidey, Jawa Barat.

Kusumasari, B. A., Kashiwaya, K., Tada, Y., Rahayudin, Y., and Koike, K., 2024, Reservoir temperature assessment by multicomponent geothermometry through a case study of Patuha Geothermal Field, Indonesia: IOP Conference Series: Earth and Environmental Science, **1383**(1), https://doi.org/10.1088/1755-1315/1383/1/012007.

Letelier, J. A., O'Sullivan, J., Reich, M., et al., 2021, Reservoir architecture model and heat transfer modes in the El Tatio-La Torta geothermal system, Central Andes of northern Chile: Geothermics, **89**(July 2020), 101940, https://doi.org/10.1016/j.geothermics.2020.101940.

Mahboob, M. A., Celik, T., and Genc, B., 2024, Predictive modelling of mineral prospectivity using satellite remote sensing and machine learning algorithms: Remote Sensing Applications: Society and Environment, **36**(July), 101316, https://doi.org/10.1016/j.rsase.2024.101316.

Medici, G., Ling, F., and Shang, J., 2023, Review of discrete fracture network characterization for geothermal energy extraction: Frontiers in Earth Science, **11**(December), 1–17,

https://doi.org/10.3389/feart.2023.1328397.

Miao, F., Yao, L., and Zhao, X., 2021, Evolving convolutional neural networks by symbiotic organisms search algorithm for image classification: Applied Soft Computing, **109**, 107537, https://doi.org/10.1016/j.asoc.2021.107537.

Mishra, R. K., Reddy, G. Y. S., and Pathak, H., 2021, The understanding of deep learning: A comprehensive review: Mathematical Problems in Engineering, 1-15, https://doi.org/10.1155/2021/5548884.

Mordensky, S. P., Lipor, J. J., DeAngelo, J., Burns, E. R., and Lindsey, C. R., 2022, Predicting geothermal favorability in the Western United States by using machine learning: Addressing challenges and developing solutions: Proceedings, 47th workshop on geothermal reservoir engineering, Stanford University, February 7-9.

Mulugeta, B. D., Fujimitsu, Y., Nishijima, J., and Saibi, H., 2021, Interpretation of gravity data to delineate the subsurface structures and reservoir geometry of the Aluto–Langano geothermal field, Ethiopia: Geothermics, **94**(July), 102093, https://doi.org/10.1016/j.geothermics.2021.102093.

Muzaky, H., and Jaelani, L. M., 2019, Analysis of the impact of land cover on surface temperature distribution: Urban heat island studies in Medan and Makassar: IOP Conference Series: Earth and Environmental Science, **389**(1), https://doi.org/10.1088/1755-1315/389/1/012047.

Nigussie, W., Alemu, A., Mickus, K., et al., 2023, Subsurface structural control of geothermal resources in a magmatic rift: gravity and magnetic study of the Tulu Moye geothermal prospect, Main Ethiopian Rift: Frontiers in Earth Science, **11**(July), 1–19, https://doi.org/10.3389/feart.2023.1181533.

Novaes, M. P., Carvalho, L. F., Lloret, J., and Proença, M. L., 2021, Adversarial deep learning approach detection and defense against DDoS attacks in SDN environments: Future Generation Computer Systems, **125**, 156–167, https://doi.org/10.1016/j.future.2021.06.047.

Oskooi, B., Mohammadi, B., and Mirzaei, M., 2014, A study on the geothermal reservoirs in Mahallat area, Markazi Province by 1D and 2D inversion of the magnetotelluric data: Iranian Journal of Geophysics, **8**(2), 10–25 (in Persian).

Prasetya, S. R., 2024, Compounding Multi-Hazard Impact Assessment of Volcanic and Cyclone Hazards : A Case Study from Saint Vincent: M.Sc. thesis, University of Twente.

Putra, D. P. N., 2021, Integrasi Data Metode Gayaberat dan Audio Magnetotelurik Menggunakan Simultaneous Joint Inversion Untuk Identifikasi Sesar di Lapangan "X.": Undergraduate thesis, Institut Teknologi Sepuluh Nopember.

Putra, D. P. N., 2024, Optimasi Rekonstruksi Pemetaan Geologi Berdasarkan Model Gayaberat Satelit dan Data Citra Satelit Menggunakan Algoritma Machine Learning untuk Monitoring Lingkungan Sumber Daya Panas Bumi: M.Sc. thesis, Institut Teknologi Sepuluh Nopember.

Putra, D. P. N., Fajar, M. H. M., Warnana, D. D., Widodo, A., Ulumuddin, F., and Zukhrufah, S. Z., 2023, Subsurface analysis on Ranu Grati Lineaments with satellite gravity data: Jurnal Penelitian Pendidikan IPA, **9**(10), 8462–8466, https://doi.org/10.29303/jppipa.v9i10.3400.

Putra, D. P. N., Utama, W., Garini, S. A., and Indriani, R. F., 2024, Geological mapping optimisation using satellite gravity, satellite imagery, and seismic

shear velocity (Vs30) to monitor lithological condition in geothermal area of Mount Salak, West Java: BIO Web of Conferences, **89**, https://doi.org/10.1051/bioconf/20248902001.

Puzyrev, V., 2019, Deep learning electromagnetic inversion with convolutional neural networks: Geophysical Journal International, **218**(2), 817–832, https://doi.org/10.1093/gji/ggz204.

Qian, C., Tong, M., Yu, X., and Zhuang, S., 2021, CNN-based visual processing approach for biological sample microinjection systems: Neurocomputing, **459**, 70–80, https://doi.org/10.1016/j.neucom.2021.06.085.

Rahayudin, Y., Kashiwaya, K., Tada, Y., Iskandar, I., Koike, K., Atmaja, R. W., and Herdianita, N. R., 2020, On the origin and evolution of geothermal fluids in the Patuha Geothermal Field, Indonesia based on geochemical and stable isotope data: Applied Geochemistry, **114**(January 2020), 104530, https://doi.org/10.1016/j.apgeochem.2020.104530.

Ramadhan, Y., Chandra, V. R., Akmala, I., Sesesega, R. S., Iskandar, C., and Wijaya, R., 2022, The antithetic concept of structure system in Patuha Geothermal Field compared to other fields in West Java: Proceedings PIT IAGI 51st 2022 Makassr, South Sulawest, October 2022.

Ratman, N., and Gafoer, S., 1998, Peta Geologi Lembar Jawa bagian Barat: Pusat Penelitian dan Pengembangan Geologi, Badan Geologi, KESDM Republik Indonesia.

Reski, E., Amin, T. Al, Ramadhan, Y., Atmaja, R. W., and Wilmarth, M., 2024, Structural model update on the Patuha geothermal system, West Java, Indonesia: IOP conference series: Earth and Environmental Science, **1293**(1), https://doi.org/10.1088/1755-1315/1293/1/012005.

Riefolo, C., Belmonte, A., Quarto, R., Quarto, F., Ruggieri, S., and Castrignanò, A., 2022, Potential of GPR data fusion with hyperspectral data for precision agriculture of the future: Computers and Electronics in Agriculture, **199**(February), https://doi.org/10.1016/j.compag.2022.107109.

Saadi, S. B., Sarshar, N. T., Sadeghi, S., Ranjbarzadeh, R., Forooshani, M. K., and Bendechache, M., 2022, Investigation of effectiveness of shuffled frog-leaping optimizer in training a convolution neural network: Journal of Healthcare Engineering, 2022, https://doi.org/10.1155/2022/4703682

Sang, X., Xue, L., Ran, X., Li, X., Liu, J., and Liu, Z., 2020, Intelligent high-resolution geological mapping based on SLIC-CNN: ISPRS International Journal of Geo-Information, **9**(2), https://doi.org/10.3390/ijgi9020099.

Schrott, L., and Sass, O., 2008, Application of field geophysics in geomorphology: Advances and limitations exemplified by case studies: Geomorphology, **93**(1–2), 55–73, https://doi.org/10.1016/j.geomorph.2006.12.024.

Segoni, S., Pappafico, G., Luti, T., and Catani, F., 2020, Landslide susceptibility assessment in complex geological settings: sensitivity to geological information and insights on its parameterization: Landslides, **17**(10), 2443–2453, https://doi.org/10.1007/s10346-019-01340-2.

Shah, A., Shah, M., Pandya, A., Sushra, R., Sushra, R., Mehta, M., Patel, K., and Patel, K., 2023, A comprehensive study on skin cancer detection using artificial neural network (ANN) and convolutional neural network (CNN): Clinical EHealth, **6**, 76–84,

https://doi.org/10.1016/j.ceh.2023.08.002.

Shirmard, H., Farahbakhsh, E., Müller, R. D., and Chandra, R., 2022, A review of machine learning in processing remote sensing data for mineral exploration: Remote Sensing of Environment, **268**(February 2021), 112750, https://doi.org/10.1016/j.rse.2021.112750.

Silva-Fragoso, A., Norini, G., Nappi, R., Groppelli, G., and Michetti, A. M., 2024, Improving the accuracy of digital terrain models using drone-based LiDAR for the morpho-structural analysis of active calderas: The case of Ischia Island, Italy: Remote Sensing, **16**(11), https://doi.org/10.3390/rs16111899.

Singh, D., and Singh, B., 2020, Investigating the impact of data normalization on classification performance: Applied Soft Computing, **97**, 105524, https://doi.org/10.1016/j.asoc.2019.105524.

Sondakh, G. G., 2022, Life Cycle Assessment of The Geothermal Power Plant in The Patuha Geothermal Field, Indonesia: M.Sc. thesis, Reykjavík University, https://en.ru.is/ise/research/research-projects/life-cycle-assessment-of-the-geothermal-power-plant-in-the-patuha-geothermal-field-indonesia.

Su, S., Zhao, G., Xiao, W., Yang, Y., and Cao, X., 2021, An image-based approach to predict instantaneous cutting forces using convolutional neural networks in end milling operation: International Journal of Advanced Manufacturing Technology, **115**(5–6), 1657–1669, https://doi.org/10.1007/s00170-021-07156-6.

Thiele, S. T., Zimik, H. V., Samsu, A., Akhtar, S., Kamath, A., and Khanna, P., 2024, Outcrop analogue constraints on subsurface reservoir properties of the Puga geothermal field, NW Himalaya: Geothermics, **123**(July), 103099, https://doi.org/10.1016/j.geothermics.2024.103099.

Tut Haklidir, F. S., and Haklidir, M., 2020, Prediction of reservoir temperatures using hydrogeochemical data, Western Anatolia geothermal systems (Turkey): A machine learning approach: Natural Resources Research, **29**(4), 2333–2346, https://doi.org/10.1007/s11053-019-09596-0.

United States Geological Survey, 2013, Landsat 8 band designations, 26–29, https://www.usgs.gov/media/images/landsat-8-band-designations.

Utama, W., Hermana, M., Anjasmara, I. M., Indriani, R. F., Garini, S. A., Pratama, D., and Putra, N., 2024, Towards improving sustainable water management in geothermal fields : SVM and RF land use monitoring: Journal of Human, Earth, and Future, 5(2), https://doi.org/10.28991/HEF-2024-05-02-06.

Utama, W., Putra, D. P. N., Garini, S. A., and Indriani, R. F., 2023, Optimizing surface lithology interpretation from global gravity model and Landsat 8 satellite imagery in Semeru Mountain, Indonesia: IOP conference series: Earth and Environmental Science, **1276**(1), https://doi.org/10.1088/1755-1315/1276/1/012048.

Utama, W., Putra, D. P. N., Indriani, R. F., and Garini, S. A., 2023, Subsurface identification using resistivity method for infrastructure planning in Benowo Area, Surabaya City: IOP Conference Series: Earth and Environmental Science, **1250**(1), https://doi.org/10.1088/1755-1315/1250/1/012018.

Vu, M. T., and Jardani, A., 2021, Convolutional neural networks with SegNet architecture applied to three-dimensional tomography of subsurface

electrical resistivity: CNN-3D-ERT: Geophysical Journal International, **225**(2), 1319–1331, https://doi.org/10.1093/gji/ggab024.

Wagner, F. M., and Uhlemann, S., 2021, An overview of multimethod imaging approaches in environmental geophysics: Advances in Geophysics, **62**(3), 1–72, https://doi.org/10.1016/bs.agph.2021.06.001.

Wang, Y., and Pang, Z., 2023, Heat flux in volcanic and geothermal areas: Methods, principles, applications and future directions: Gondwana Research, **122**, 260–278, https://doi.org/10.1016/j.gr.2022.09.010.

Wang, W., Xue, C., Zhao, J., Yuan, C., and Tang, J., 2024, Machine learning-based field geological mapping: A new exploration of geological survey data acquisition strategy: Ore Geology Reviews, **166** (January), 105959, https://doi.org/10.1016/j.oregeorev.2024.105959.

Xu, Z., Xiao, T., He, W., Wang, Y., and Jiang, Z., 2023, Spatial knowledge-infused hierarchical learning: An application in flood mapping on Earth imagery: GIS*:* Proceedings of the ACM International Symposium on Advances in Geographic Information Systems, **1**(1), Association for Computing Machinery, https://doi.org/10.1145/3589132.3625591.

Yusroni, S. A., Kemalasari, V. T., and Putra, D. P. N., 2021, Identification of land cover changes from Landsat 8 Oli Satellite imagery using normalized difference vegetation index (Ndvi) method (Study case: Surabaya): Journal of Marine-Earth Science and Technology, **2**(1), 5–10, https://doi.org/10.12962/j27745449.v2i1.74.

Zhang, Q., Zhang, M., Chen, T., Sun, Z., Ma, Y., and Yu, B., 2019, Recent advances in convolutional neural network acceleration: Neurocomputing, **323**, 37–51, https://doi.org/10.1016/j.neucom.2018.09.038.

Zhao, B., Zhang, X., Li, H., and Yang, Z., 2020, Intelligent fault diagnosis of rolling bearings based on normalized CNN considering data imbalance and variable working conditions: Knowledge-Based Systems, **199**, 105971, https://doi.org/10.1016/j.knosys.2020.105971.